International Journal of Chemical and Biochemical Sciences
(ISSN 2226-9614)

Journal Home page: www.iscientific.org/Journal.html

Zeolite: review of characterization and applications

Ho Soonmin

Faculty of Health and Life Sciences, INTI International University, 71800, Putra Nilai, Negeri Sembilan, Malaysia.

Abstract

There are two types of zeolites, namely natural and synthetic zeolite. Several techniques have been used to prepare zeolite, such as hydrothermal, solvothermal, microwave-assisted method, and ionothermal techniques. The prepared zeolite could be used in water purification, adsorption processes, ion exchangers, agricultural fields, air purification, and catalysis applications. The physical properties of the obtained zeolites were investigated using scanning electron microscopy, atomic force microscopy, Fourier transform infrared spectroscopy, the x-ray diffraction technique, thermogravimetric analysis, and X-ray fluorescence spectroscopy. Experimental findings revealed that the adsorption capacity of dyes, heavy metals, and phenol compounds is strongly dependent on the conditions. In addition, zeolite was modified with metal elements to improve quality and adsorption performance. It was noted that zeolite showed a negative charge and was able to remove cationic species but was very hard to remove anionic species in wastewater treatment. Adsorption data were studied using Langmuir, Temkin, and Freundlich isotherm models, while the kinetic study was measured through pseudo-first-order and pseudo-second-order models.

Keywords: wastewater treatment, pollution, Zeolite, adsorbent, surface area, air purification, catalysts, water treatment

Full length article *Corresponding Author, e-mail: soonmin.ho@newinti.edu.my

1. Introduction

Zeolite has been used in gas separation, wastewater treatment, ion exchange, and catalysis due to its unique structural properties [1, 2]. In general, zeolite could be identified as natural zeolite or synthetic zeolite [3, 4]. Natural zeolite is a hydrated aluminosilicate material, can be observed in rocks and volcanic origin [5, 6]. Table 1 shows the physical properties of some natural zeolites. Currently, more than 150 zeolites are synthesized via the slow crystallization process [7] due to high demand. Zeolite has a three-dimensional crystalline [8], microporous [9], rigid structure, and contains oxygen, silicon, and aluminium [10]. Moreover, aluminum and silicon atoms were tetrahedrally coordinated through shared oxygen [11]. Obviously, crystals serve as molecular sieves due to the channel sizes [12] and the pores are nearly uniform. Advantages of zeolites include no disposal problems [13], less time for softening, no corrosion issues [14], and high thermostability [15]. However, there are some limitations, such as low catalytic site density [16], treated water consisting of more salts [17], and the health issue of inhaled zeolite dust [18]. China is the largest manufacturer of natural zeolite, followed by South Korea and Slovakia. Nowadays, several zeolite companies such as Zeolyst International, Clariant, KMI zeolite Inc, Zeocem, Tosoh, Grace, Resonac Corporate, Chemiewerk Bad Kostritz GmbH and Huiying Chemical Industry (Xiamen) Co. Ltd provide high-performance products to consumers.

Currently, numerous adsorbents have been reported for the removal of pollutants in wastewater treatment. Activated carbon was synthesized using carbonization process [19], physical activation, and chemical activation techniques [20]. Sometimes, annealing and activating agents have been employed for better pore development and improved adsorption capacity [21]. The prepared activated carbon displayed a higher surface area, high hydrophobicity, and a well-developed porosity structure [22]. On the other hand, fly ash [23], layered double hydroxide [24], and bentonite [25] have been chosen to adsorb undesired materials.

In this work, various techniques have been used to prepare zeolite. The properties of prepared zeolite were studied using scanning electron microscopy (SEM), X-ray fluorescence spectroscopy (XRF), Fourier transform infrared spectroscopy (FTIR), thermogravimetric analysis (TGA), and x-ray diffraction technique (XRD). The removal efficiency of dye compounds, phenol compounds, heavy metal, and carbon dioxide gas was investigated. The adsorption data was measured through various types of isotherms (Langmuir model, pseudo first-order model, Freundlich isotherm, pseudo second-order models, and Temkin isotherm).

2. Removal of various types of pollutants using zeolite

The obtained experimental findings [26] reflected that adsorption capacity on natural chabazite (namely as CH-N) was found to be 114.989 mg/g, 19.68 mg/g and 18.716 mg/g for lead, chromium, and cadmium. The As(V) ions have

been absorbed by modified zeolite, namely CH-MS (79%) effectively removing lead, chromium, and cadmium in the range of 33 % to 67 %. According to the XRD analysis, natural zeolite showed several diffraction peaks such as 9.39°, 20.43° and 30.37°, while the modification process takes place only on the external surface and crystalline structure will remain. In the FTIR studies, natural zeolite displayed higher intensities (1640 cm^{-1}, 3600 $cm^{-1}$and 3380 cm^{-1}) if compared to modified samples due to the higher water content. While modified zeolite indicated a typical band at 3640 cm^{-1} (hydroxyl group). According to thermogravimetric (TGA) analysis (figure 1), the weight of prepared adsorbents reduced significantly when the temperature was increased up to 600 °C. A higher deduction could be observed in modified zeolite (19.92 %) than in natural zeolite (16.55 %). In differential analysis (DTG), water loss could be identified in two steps, namely humidity loss (81 °C) and loss of water (118 °C). Also, the decomposition of calcium carbonate could be seen at 270 °C. Other results have been highlighted in Table 2. Ciprofloxacin is employed for treating bacterial infections such as diarrhea, bone, typhoid fever, skin infection, and joint infection. However, the residual ciprofloxacin can cause harm to human health and ecosystems. Researchers have pointed out that conventional techniques (biological treatments, ozonation, and oxidation) were unable to remove ciprofloxacin effectively because of the stable chemical structure of ciprofloxacin. Ciprofloxacin has two groups [27], namely the carboxyl group (pKa=8.89) and the amine group (pKa=5.9). In general, it could exist in three forms (figure 2), namely cation (pH 3-6), anion (pH 9-12), and zwitterion (pH 6-9) strongly dependent on the pH value. Iron (5%) was added to 5A zeolite via the ozonation process [28]. A smooth surface, pore size of 0.5 nm, porous structure, and surface area of 93.25 m^2/g (figure 3) were reported. The highest adsorption capacity in UV/O_3/Fe-Z5A (73.4 %) if compared to O_3 (49.3 %), O_3/UV (57.1 %) and O_3/Fe-Z5A (65.6 %). It was noted that more ozone will be consumed in the synergic process. Also, it is worth mentioning that UV/O_3 has a higher removal efficiency than ozone alone because UV rays can produce active oxygen species. Table 3 shows the removal efficiency of ciprofloxacin using various types of adsorbents.

Chitosan is a nontoxic fibrous substance, usually from the outer skeleton of shrimp, lobster, and crab [39]. It was employed in drug production and medicine manufacturing. Also, it could help blood clot and reduce the uptake of fat from foods. It was noted that the degradation of chitosan depended on several factors, such as the physical method, the chemical technique and the type of enzyme used. Endar and co-workers [40] have reported that chitosan (mixed with acetic acid in a ratio of 1:1) was cross-linked with zeolite to remove methylene blue. The characterization part was studied using SEM (adhesive structure, porous morphology, had interlayers), EDX (carbon=3.11 %, oxygen=45.37 %, sodium=12.69 %, aluminum=7.99 %, silica=30.84 %), FTIR (peaks at 1011 cm^{-1}, 1423 cm^{-1}, 1645 cm^{-1} and 3332 cm^{-1}) and pH zero-point charge (pH=9.2). According to the adsorption data, the pseudo-second-order model (R^2=0.9978) and Freundlich isotherm (R^2=0.9926) were matched to the adsorption process. In addition, the obtained results confirmed that the removal percentage was 97% (adsorption capacity=242.51 mg/g) at pH 10, for 1 hour. Radoor and co-workers [41] have used bio-polymer poly(diallyl dimethyl ammonium chloride) to modify the ZSM-5 zeolite for removing cationic dyes. This modified zeolite showed a larger pore diameter and higher surface area based on the TEM, SEM, and nitrogen adsorption analysis. The highest adsorption capacity was 4.31 mg/g (time= 300 minutes, adsorbent dose=0.1g, initial dye concentration=10 mg/L, pH=10, temperature=30 °C). Adsorption data could be described using a pseudo-second-order model and the Freundlich isotherm. In the reusability studies, the obtained adsorbent can be employed at least six times without loss in the percentage of removal. Zeolite-X (particle size=0.45 nm) was used to absorb dye from textile wastewater [42]. The highest removal efficiency reached 97.77 % in the highlighted conditions (pH=4, time=60 minutes, adsorbent dose=0.4 g). The FTIR technique has been used to determine several functional groups, such as OH stretching vibration (3854 cm^{-1}), OH adsorbed water (3447 cm^{-1}), Al-OH stretching (3650 cm^{-1}), C=C bond (1400 cm^{-1}), Si-O-Si stretching (1094 cm^{-1}) and symmetric Si-O-Si stretching (809 cm^{-1}). In the XRD analysis, several diffraction peaks could be observed at 6°, 11.94°, 23.1°, 25.52° and 28.94°. These broad peaks represented amorphous phases with a microporous structure.

Chromium has the symbol “Cr” and an atomic number of 24. It has been reported that chromium showed complex chemistry [43], displayed different oxidation states (from +6 to -2). Several industries, such as the energy sector, metal production, chemical manufacturing, wood production, tanning, and dyeing processing, release chromium compounds into water and air. Chromium (VI) ions have been identified as carcinogenic to humans due to respiratory disorders, internal haemorrhage, kidney, and liver damage. Physical properties of clinoptilolite, such as solid density (2.1 g/cm^3), particle size (0.68 mm), packing density (2.25 g/cm3), total surface area (800 m^2/g) and cation exchange capacity (2.5 meq/g) were reported [44]. Experimental findings confirmed if higher chromium ion adsorption capacity in zeolite treated with NaCl (4.5 mg/g) if compared to as received (2.2 mg/g) zeolite. Also, more bed volume and a longer breakthrough time could be seen in treated NaCl samples (64 bed volume, 1500 minutes). Based on the TEM images, lamellar-shaped particles can be seen in figure 4c. The composition of the clinoptilolite was studied using the x-ray fluorescence technique. Major elements such as SiO_2 (73 %) and Al_2O_3 (12 %) were detected, while some trace elements, included CaO (2.1%),K_2O (6.7 %), MgO (1.9 %), and Fe_2O_3 (4.3 %) were also observed. According to the FTIR studies, several peaks at 3400, 1640 cm^{-1} (water), 1100 cm^{-1} (SiO_4 tetrahedral), 1000 cm^{-1} (Al-O), 750-700 cm^{-1} (SiO_4 symmetric vibration) were found in the prepared samples. Kouli and co-workers [45] have reported that chromium removal percentage increases when the contact time (1 hour to 6 hours) is increased for the different concentrations of zeolites, such as 1g/L (42 % to 63 %), 2g/L (46 % to 79 %), 5 g/L (54 % to 75 %), 10 g/L (63 % to 79 %) and 20 g/L (75 % to 79 %), respectively. Based on the SEM images, different results could be observed in pure zeolite-X (uniform spheroidal cubic, greyish-black color, average diameter was less than 10 μm) and pure magnetite (bright black, size=40 to 70 nm).

Table 1. Physical properties of several types of natural zeolites.

Zeolite	Porosity (%)	Exchange capacity (meq/g)	Specific gravity (g/cm^3)	Bulk density (g/cm^3)	Heat stability
analcime	18	4.54	2.24 to 2.29	1.85	High
chabazite	47	3.84	2.05 to 2.1	1.45	High
heulandite	39	2.91	2.18 to 2.2	1.69	Low
mordenite	28	4.29	2.12 to 2.15	1.7	High
philipsite	31	3.31	2.15 to 2.2	1.58	Moderate
clinoptilolite	34	2.16	2.15 to 2.25	1.15	High
erionite	35	3.12	2.02 to 2.08	1.51	High

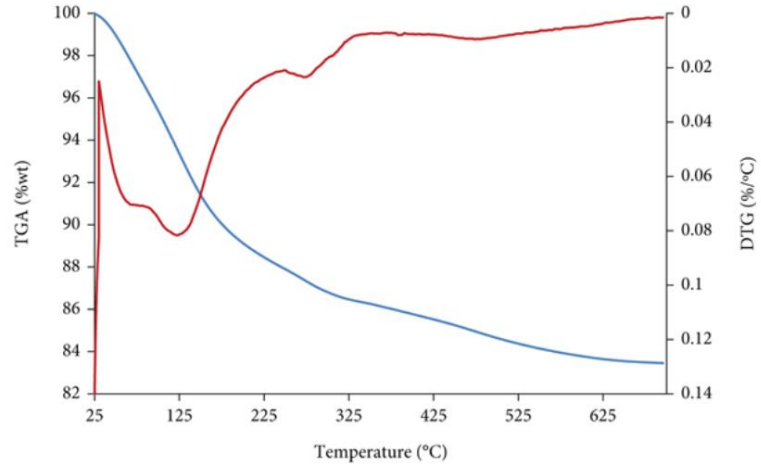

(a)

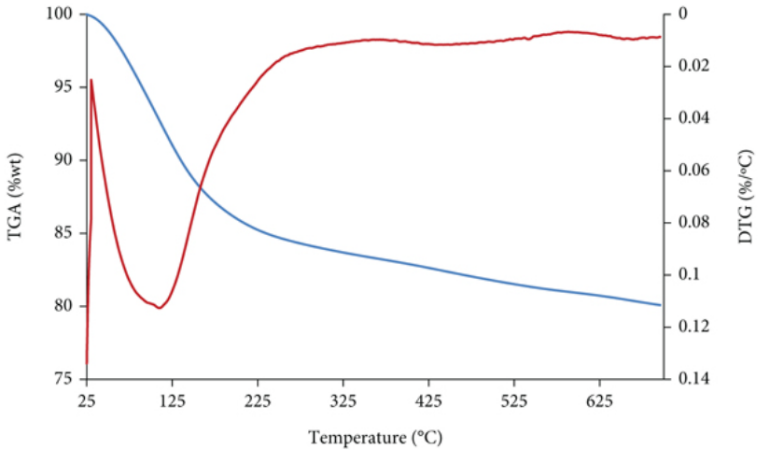

(b)

Figure 1: TGA and DTG analysis of (a) CH-N zeolite (b) CH-MS zeolite [26]

Table 2: Textural properties of the prepared zeolite.

	Natural zeolite	Modified zeolite
Surface area ($^{m2/}$g)	324.2	325.9
Pore diameter (nm)	2.94	3.04
Pore volume (cm^3/g)	0.198	0.216
Morphological studies	Well-defined structure, rhombohedral crystals	Partially rhombohedral structures
EDX studies	Fe=3.76 % Ca=5.95 % Mg=4.31 % K=3.12 % Si=60.11 % Na=3.65 % Al=18.22 % Others=0.88 %	Fe=3.75 % Ca=0 % Mg=3.98 % K=3 % Si=64.65 % Na=0 % Al=24.1 % Others=0.52 %

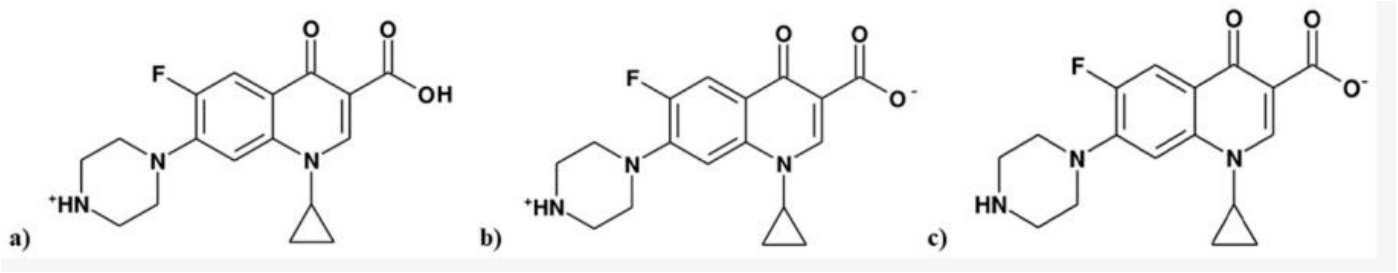

Figure 2: Several types of ciprofloxacin such as cationic (a), zwitterionic (b) and anionic (c) were reported [27]

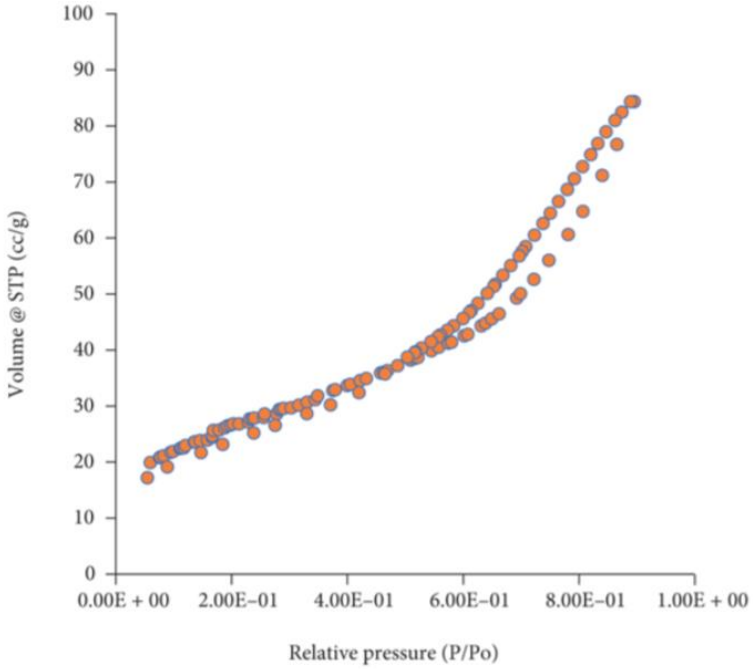

Figure 3: BET isotherm for Fe-zeolite A [28]

Table 3: Removal of ciprofloxacin using different types of adsorbents.

Adsorbent	Removal efficiency (%)	Conditions	Researchers
Nano-sized magnetite [29]	80	Time=24 hours, pH=5.97, adsorbent dose=10 g/dm^3, initial concentration=33 mg/dm^3	Rakshit and co-workers, 2013
Graphene hydrogel [30]	75	Initial concentration=50 mg/dm^3, temperature=25 °C, time=36 hours	Ma and co-workers, 2015.
Carbon from date palm leaflets [31]	56	pH=6, Initial concentration=100 mg/dm^3, adsorbent dose=2 g/dm^3, temperature=45 °C, time=48 hours	El-Shafey and co-workers, 2012.
Halloysite nanotubes [32]	95	pH=5-6, Initial concentration=30 mg/dm^3, adsorbent dose=1.7 g/dm^3, temperature=20 °C, time=90 minutes	Cheng and co-workers, 2018.
γ-Al_2O_3 nanoparticles [33]	53	Initial concentration=20 mg/dm^3, adsorbent dose=0.775g/dm^3, pH=7.5, time=46.25 minutes	Najafpoor and co-workers, 2019.
Biomaterials from banyan aerial roots [34]	97	pH=8, Initial concentration=60 mg/dm^3, adsorbent dose=1.2 g/dm^3, temperature=25 °C, time= 48 hours	Fan and co-workers, 2020
Biochar montmorillonite [35]	86	Initial concentration=25 mg/dm^3, adsorbent dose=1 g/dm^3, pH=5-6, time=400 minutes	Ashiq and co-workers, 2019.
Coal fly ash [36]	39	Initial concentration=160 mg/dm^3, adsorbent dose=40 g/dm^3, temperature=40 °C, time=100 minutes	Zhang and co-workers, 2011.
Clinoptilolite [37]	99	pH=6, Initial concentration=5 mg/dm^3, adsorbent dose=2 g/dm^3, temperature=25 °C	Ngeno and co-workers, 2019.
Synthesized zeolites (A,X,Y) [38]	27-61.4	adsorbent dose=0.5 g/dm^3, Initial concentration =150 mg/dm^3, pH=3	Zide and co-workers, 2018.

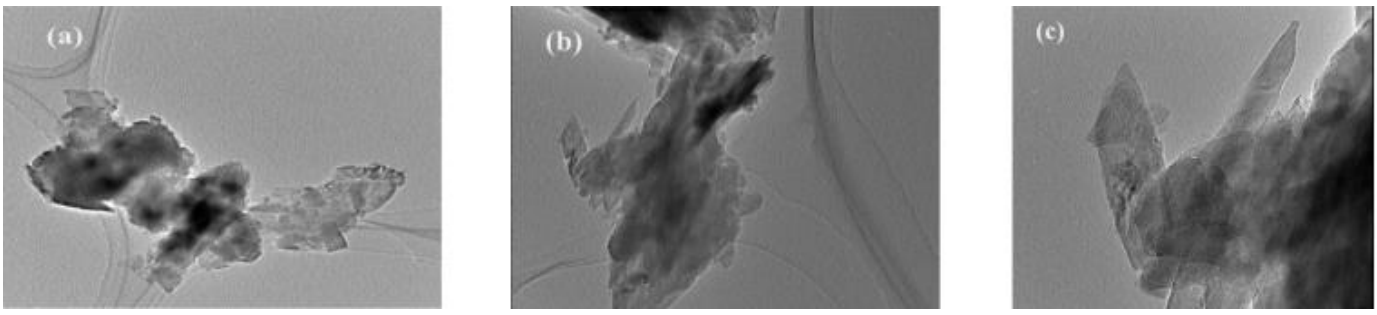

Figure 4: TEM images before pretreatment (a) after pretreatment (b) and after adsorption process (c) for clinoptilolite [44]

Table 4: Several techniques have been used to remove chromium ions.

Method	Experimental results
Chemical reduction	Removal of chromium ions [46] has increased with increasing doses from 0.25 (45%), 0.5 (85%), 0.75 (88%) and 1 mg/L (92%) at initial chromium concentration of 50 µg/L. Experimental results confirmed that the concentration was less than 10 µg/L in treated water through continuous flow treatment using sand filtration.
electrocoagulation	The removal of chromium [47] ions from electroplating wastewater was found to be low (pH<2), it increased when the pH was 4, remained high (pH 4-8), finally dropped when the pH was more than 8. Removal rate increases when the current densities are increased from 10-40 mA/cm^2 in specific conditions (concentration of chromium was 800 mg/L, pH=7.5). The percentage of removal reached 99% after 40 minutes.
Bacterial remediation capabilities	Over 90 % Cr(VI) removal could be observed using bio-reduction and bio-precipitation (Bacillus cereus and Enterococcus sp), after 45 days, through a continuous feed of 40 mg/L-60 mg/L [48]. Cr(VI) ions have been reduced to Cr (III) ions through anaerobic conditions.
Biosorption	Seven bacterial strains have been isolated from tanning processing wastes [49]. They observed that a highly significant positive and negative correlation value could be found between Cr (VI) removal by strains.
Bioaccumulation	Srinath and co-workers [50] have observed that *Bacillus circulans* (34.5 mgCr/g) and *Bacillus megaterium (32 mg Cr/g) were able to remove chromium ions (in 24 hours, initial concentration was 50 mgCr/L) from tannery effluent.* Raman and co-workers have investigated the bioremediation *Stenotrophomonas maltophilia* isolated from tannery wastewater. The obtained results reflected that the chromium ion bioaccumulation rate was higher if compared to reduction.
Adsorption	Fly ash [51] was treated with concentrated sulfuric acid and heat conditions (150 °C for 24 hours). The highest adsorption capacity reached 21 mg/g at pH 1-3.
Adsorption	The percentage of removal was found to be 40.04 % and 0.34 % at pH 3 and pH 10, respectively. Based on the XPS analysis [52], 78.8% of the chromium absorbed on the wood-based powdered activated carbon was in trivalent states. Several types of functional groups (C=O, C-OH) were presented.
Membrane filtration	Adsorption data were supported by the Langmuir model and pseudo-second-order-kinetic isotherm [53]. Adsorption capacity was 14.451 mg/g (batch system) and 14.104 mg/g (continuous in-flow system) as reported when chitosan-coated iron oxide immobilized hydrophilic poly(vinylidene) fluoride membrane was used. Competing ions ($PO_4^{3-}, Cl^-, NO_3^- and SO_4^{2-}$) will not affect the removal efficiency.

Table 5: Properties of nano zeolite and copper supported nano zeolite.

	Nano zeolite	Copper supported nano zeolite
Surface area (m^2/g)	680	890
Pore volume (cm^3/g)	0.271	0.18
XRD diffraction peaks	7°-9° and 23°-25°	35.6° and 38.9°

Table 6: Removal of 2-chlorophenol using different types of adsorbents.

Absorbent	Adsorption capacity (mg/g)	Researchers
Activated carbon fibers [62]	141	Ozgur and Ferhan, 2009
Surfactant modified bentonite [63]	50	Rawajfih and Nsour, 2006
Graphene zirconiumoxide [64]	140	Rao and co-workers, 2014
Surfactant modified natural zeolite [65]	12.7	Kuleyin, 2007
Bagasse fly ash [66]	52.52	Shah and co-workers, 2011

Table 7: Malachite green dye compounds removal ability using different adsorbents.

Adsorbent	Adsorption capacity (mg/g)	Researchers
Jute fiber carbon [69]	136.6	Porkodi and Kumar, 2007
Rice husk derived biochar modified [70]	373.02	Tsai and co-workers, 2022
Bamboo pulp black liquor based activated carbon [71]	847	Mengyuan and co-workers, 2022
Cyclodextrin-based adsorbent [72]	91.9	Crini and co-workers, 2007
Wood apple shell [73]	80.645	Ashish and co-workers, 2017
Sugarcane baggase particels [74]	190	Nilay and Barun, 2013
Montmorillonite [75]	262.494	Baybars, 2016
degreased coffee beans [76]	24.8 to 55.3	Baek and co-workers, 2010
Untreated oil palm empty fruit bunch [77]	714.3	Rohani and co-workers, 2021
Reduced graphene oxide [78]	279.85	Dibya and Hara, 2021
Catha edulis stem based activated carbon [79]	5.6	Abate and co-workers, 2020
Rumex abyssinicus derived activated carbon [80]	98.43	Abewaa and co-workers, 2023
Teak leaf litter powder [81]	333.33	Oyelude and co-workers, 2018
Rubber wood sawdust [82]	27.4	Linh and co-workers, 2012
Lemon peel based activated carbon [83]	66.67	Sayed and co-workers, 2014
Apricot stone based activated carbon [84]	23.8-88.05	Abbas, 2020

Experimental results confirmed that magnetite with zeolite-X displayed higher magnetic fields (more than 1.5 T) and 29 Am^2/kg based on the mass magnetization saturation. While pure magnetite showed 70 Am^2/kg (saturated mass magnetization) and lower magnetic fields (less than 1.5 T). Table 4 shows several strategies that have been employed for chromium pollution remediation, such as ion exchange, precipitation, adsorption, electrocoagulation, chemical reduction method, and biological reduction. Nickel has the symbol "Ni", and atomic number of 28. In general, this element is a hard, silvery-white metal. Exposure to nickel may cause allergies, lung fibrosis, nasal cancer, cardiovascular and kidney diseases. Phosphoric acid has been used to treat the HZSM-5 zeolite [54] in the mentioned conditions (60 °C, 180 minutes) and showed a surface area of 422 m^2/g. A higher uptake of nickel ions could be seen in this zeolite than sodium modified zeolite (surface area=385 m^2/g) because of the more exchangeable sodium ion. Experimental results confirmed that percentage removal increased when the pH was increased (3 to 4). However, precipitation was formed when the pH was greater than 4. Adsorption data were described using the Langmuir model (maximum capacity was 39.96 mg/g) and pseudo-second-order model in both zeolites. NaCl was used to treat Jordanian zeolite tuff, as reported [55]. According to the XRF investigations, the major elements are SiO_2 (35.63 %), Fe_2O_3 (11.71 %), MgO (11.27 %), Al_2O_3 (9.71 %), and CaO (6.65 %). While some trace elements such as TiO (1.73 %), Na_2O (1.42 %), K_2O (1.29 %), P_2O_5 (0.53 %) and MnO (0.12 %). Experimental findings confirmed that adsorption capacity decreased when the particle size was increased from 45 μm-90 μm (1.005 meq/g), 90 μm-180 μm (0.681 meq/g), 180 μm-355 μm (0.409 meq/g), to 355-710 μm (0.358 meq/g). It is shown that a higher correlation coefficient (R^2=0.991) was found in the Langmuir isotherm. On the other hand, bentonite was employed to treat Jordanian zeolite (philipsite) [56]. The adsorption process is a spontaneous reaction, and the adsorption capacity reached 33 mg/g (Langmuir model, R^2=0.967). Zeolite-Y membrane was

synthesized using the hydrothermal technique and successfully reduced the concentration of nickel ions [57]. The highest adsorption capacity reached 126.2 mg/g within 3 hours. The adsorption mechanism was best fitted to the Freundlich isotherm and pseudo-second-order model (R^2=0.9996). Peng and co-workers have reported the formation of coordination bonds between the nickel ions and the adsorbent based on XPS results. Experimental results highlighted that pH could affect the adsorption process in β-zeolite and β-zeolite-ethylenediamine. It was noted that the adsorption process was spontaneous, endothermic, and obeyed the pseudo-second-order kinetic model. Sadat and co-workers have pointed out that the highest nickel uptake could be observed in specific conditions (initial concentration=10-15 mg/L, pH=4.8-6, time=56-68 minutes, adsorbent dose=0.37-0.43 g/L). In organic chemistry, when hydroxyl groups are bonded to aromatic groups, it is called phenol. It is a white solid with the molecular formula C_6H_5OH. This substance may cause seizures, dermatitis, lung edema, dysrhythmia, liver, and kidney damage. Zeolite (NaP1) is prepared using fly ash and sodium hydroxide via a hydrothermal process [58]. Several elements could be found, such as sodium (0.18 %), aluminium (21.52 %), silicon (47.4 %), potassium (5.65 %), iron (14.71 %), copper (0.06 %), calcium (2.96 %) and magnesium (0.8 %). When chitosan was employed for the synthesis of zeolite, this product was called NaP1CS. Physical properties including surface area, total pore volume, and average pore width were found to be 98.5 m^2/g, 0.302 cm^3/g, 11.38 nm and 53.5 m^2/g, 0.134 cm^3/g, 11.17 nm, respectively, in NaP1 and NaP1CS. Functional group in the NaP1 sample was studied using FTIR technique and some peaks at 1638 cm^{-1} (bending vibration of water), 3420 cm^{-1} (O-H stretching vibration), 977 cm^{-1} (Si-O-Si), 1000-1100 cm^{-1} (C-O-C), and 1600-1650 cm^{-1} (N-H) could be seen. It is noticed that there are different thermogravimetric analysis (TGA) results in NaP1CS and NaP1. Obviously, there are two weight losses at 40 °C-120 °C and 300 °C-450 °C due to the evaporation of water and degradation of the saccharide ring, respectively, NaP1Cs. In NaP1 sample, water loss could be observed at 100 °C-200 °C, then remained stable. When the pH was 7, the highest adsorption capacity was found in the NaP1 sample, and the adsorption data was described using the Freundlich model (R^2=0.966). Also, enthalpy (-13.08 kJ/mol), entropy (-76.6 J/K.mol), and free energy (-6.6 to -7.4 kJ/mol) have been reported based on thermodynamic parameters. On the other hand, the highest removal of phenol was found when the pH was 6 in the NaP1CS sample, and the adsorption study data fitted well with pseudo-second-order isotherm. According to the thermodynamic parameters, enthalpy (-26.67 kJ/mol), entropy (114.3 J/K.mol), and free energy (-6.21 to -11.48 kJ/mol) were highlighted. Nonylphenol contains a phenol group bearing nine carbon tails. It can be used in laundry detergent, antioxidants, emulsifiers, lubricating oils, and solubilizers. Natural zeolite (San Luis Potosi, Mexico) was screened (1-2.5 mm) and washed with water [59]. The prepared sample contained calcium clinoptilolite (XRD data), and the percentage of aluminum and silicon were 3.85% and 27.92%, respectively (EDX data). Experimental results have proven that equilibrium will be achieved within 30 minutes using 0.4 g of zeolite. It is convenient to describe the adsorption process using the pseudo-second-order model (R^2=0.999) and the Temkin model (R^2=0.994). Ayse [60] has collected zeolite samples from the Cankiri-Corum Basin, Turkey. Based on the SEM images, high microporosity and a drusy texture could be observed. The percentage removal of phenol and 4-chlorophenol increases when the initial concentration and adsorbent dose are increased. Phenol removal efficiency was found to be 41-74 % and 45-80 % in hexadecyltrimethylammonium and benzyl tetradecyl ammonium modified zeolite, respectively (adsorbent concentration=20-100 g/L). The adsorption process was tested for various types of isotherms, and finally obeyed the Freundlich model. The preparation of copper supported nano zeolite was reported for the removal of 2-chlorophenol [61]. In the surface morphology studies, there are different results that could be seen in nano zeolite (very small particles, size=100 nm) and copper-nano zeolite. It was noticed that three steps could be observed at 50-250 °C (dehydration process), below 250 °C (dehydroxylation), 400-600 °C (no change) in copper supported nano zeolite based on the thermogravimetric analysis. Other properties of these zeolites have been listed in Table 5. The highest adsorption capacity reached 204.68 mg/g (pH=6, time=150 minutes) if compared to other adsorbents (Table 6). The Freundlich isotherm (R^2=0.999) and second-order-kinetic model (R^2=0.99) correlated well with the adsorption data. Based on the regeneration studies, the percentage of removal was maintained (about 80 %) after 9 cycles. The adsorption cost was found to be USD 0.58/g using copper supported zeolite, cheaper than activated carbon (USD 0.675/g).

Malachite green is used as a green-colored dye for paper, silk, and leather. It was banned in many countries due to mutagenicity, carcinogenicity, and teratogenicity. The 4A zeolite (surface area=35.5 m^2/g) was synthesized through the gas dehydration unit of the TFT plant [67]. Chemical components such as SiO_2 (55.39 %), Al_2O_3 (27.18 %), Na_2O (4.49 %), K_2O (1.03 %), CaO (3.34 %), P_2O_5 (0.79 %), Fe_2O_3 (4.47 %), TiO_2 (0.32 %), and MgO (2.99 %) were observed based on the X-ray fluorescence spectroscopy technique. Functional groups on the surface of the adsorbent can be studied using the FTIR technique. Several peaks at 3441 cm^{-1} (stretching vibration H-O-H), 1660 cm^{-1} (bending vibration H-O-H), 994 cm^{-1} (asymmetric stretching vibration Si-O-Si or Al-O-Al), 787 cm^{-1} (symmetric Si-O-Si), 684 cm^{-1} (stretching vibration Si-O-Al) and 464 cm^{-1} (bending vibration O-Si-O) have been identified. The point of zero charge (pHpzc) is pH 10.5, and the surface was predominantly negative if the pH was greater than pHpzc. The highest removal capacity reached 45.64 mg/g according to the Langmuir model (R^2=0.994) and followed pseudo-second-order kinetic model [R^2=0.99]. In thermodynamic studies, entropy, free energy and enthalpy were found to be 204.5 J/mol.K, -35.4 to -40.5 kJ/mol and 25.5 kJ/mol, respectively. A single phase of zeolite with a formula of $Na_{12}Al_{12}Si_{12}O_{48}$ has been produced by Moussa and co-workers [68]. Rapid adsorption could be observed and reached saturation level after 40 minutes. Adsorption capacity increased (9.8 to 43 mg/g) when the initial concentration was increased (10-45 mg/L) because of the diffusion of dye compounds to the zeolite, accelerated by the gradient of concentration. The influence of agitation speed was studied (100-500 rpm), and the highest adsorption capacity was seen at 200 rpm due to the best homogeneity and

avoided vortex process. Evaluating the fitness of adsorption data by the Langmuir model (R^2=0.999), confirmed that the highest adsorption capacity was 83.33mg/g. The performance of the prepared zeolite with other adsorbents has been highlighted based on previous works (Table 7).

3. The future prospects of zeolites

In 2021, world zeolites markets were valued at about USD 12.1 billion due to rapid urbanization, environmental regulations, and changing lifestyles. The market share value is expected to reach USD 14.1 billion in 2026. Natural zeolite can dominate the global market because of its high demand in building materials, wastewater treatment, animal feed, and soil remediation, and may replace synthetic zeolites (toxicity due to dust particle). A well-developed porosity structure and higher surface area must be studied for the removal of pollutants. Process improvement and process intensification should be carried out. Adsorption capacity should be investigated using acid-treated and basic-treated zeolites. Pilot-scale studies should be conducted using real wastewater to replace synthetic solutions.

4. Conclusions

In this work, the removal of dyes, phenol compounds, and heavy metals was studied using zeolite. Based on the obtained experimental results, natural zeolites and synthetic zeolites have been prepared in specific conditions for wastewater treatment processes. Several isotherms have been used to study the adsorption process, and the best model could be highlighted based on the experimental data. The adsorption capacity of the pollutant or undesired materials depended on the adsorbent dose, initial concentration, pH, agitation effect, and temperature.

Acknowledgements:

Author would like to thank INTI International University, Malaysia for the financial support.

References

[1] W. Zhang, J. Chen and G. Li. (2021). Research progress on NH_3-SCR mechanism of metal-supported zeolite catalysts. Journal of Fuel Chemistry and Technology. https://doi.org/10.1016/S1872-5813(21)60080-4.

[2] Y. Xu, X. Wang and M. Qin. (2022). Selective catalytic reduction of NO_x with CH_4 over zeolite catalysts: Research progress, challenges and perspectives. Journal of Environmental Chemical Engineering. https://doi.org/10.1016/j.jece.2022.107270.

[3] G. Michael, S. Emily and L. Robert. (2016). An undergraduate research experience: Synthesis, modification, and comparison of hydrophobicity of zeolites A and X. Polyhedron. 114: 42-52.

[4] S.M. Ho. (2017). Zeolites and their applications: review, in A. Peter, O. Ahmed, N. Nizam and S.M. Ho. (Eds). Zeolites: Synthesis, Characterisation & Practice. Ideal International E-Publication Pvt Ltd: India. 1-7.

[5] G. Liao, Y. He and H. Wang. (2023). Carbon neutrality enabled by structure-tailored zeolite-based nanomaterials. Device. https://doi.org/10.1016/j.device.2023.100173.

[6] G. Raman. (2023). Forecasting low framework density zeolites from synthesis descriptors using machine learning. Journal of Solid-State Chemistry. https://doi.org/10.1016/j.jssc.2023.124290.

[7] H. Raju, K. Latha and M. Shaik. (2023). Corrosion characteristics and performance of calcined and natural zeolite concretes. Materials Today: Proceedings. https://doi.org/10.1016/j.matpr.2023.08.124.

[8] S. Soon and H. Oh. (2023). A mini-review of the current progress and future challenges of zeolites for hydrogen isotopes separation through a quantum effect. International Journal of Hydrogen Energy. https://doi.org/10.1016/j.ijhydene.2023.08.241.

[9] N. Dzigita and G. Giedrius. (2016). Research into the properties of concrete modified with natural zeolite addition. Construction and Building Materials. 113, 964-969.

[10] V. Tyagi, M. Meena and M. Rana. (2023). Waste petroleum fluid catalytic cracking catalysts as a raw material for synthesizing valuable zeolites: A critical overview on potential, applications, and challenges. Sustainable Materials and Technologies. https://doi.org/10.1016/j.susmat.2023.e00733.

[11] J. Wang, H. Si and W. Bin. (2023). Harnessing zeolite catalyst for the cleavage of targeted chemical bonds in lignin. Chem Catalysis. https://doi.org/10.1016/j.checat.2023.100797.

[12] H. Lei, W. Wang and L. Wang. (2023). Synthesis and application of core-shell, hollow, yolk-shell multifunctional structure zeolites. Microporous and Mesoporous Materials. https://doi.org/10.1016/j.micromeso.2023.112766.

[13] B. Giuseppe, M. Roberto and P. Paolo. (2015). An industrial perspective on the impact of Haldor Topsøe on research and development in catalysis by zeolites. Journal of Catalysis. 328: 11-18.

[14] Y.Lin and C. Mikel. (2013). Recent progress in polycrystalline zeolite membrane research. Current Opinion in Chemical Engineering. 2: 209-216.

[15] T. Jie, S. Li and H. Xu. (2023). Research progress of structure design and acidity tuning of zeolites for the catalytic conversion of syngas. Journal of Fuel Chemistry and Technology. https://doi.org/10.1016/S1872-5813(22)60035-5.

[16] A. Babak, A. Fazel and B. Shafei. (2023). Natural zeolite as a supplementary cementitious material – A holistic review of main properties and applications. Construction and Building Materials. https://doi.org/10.1016/j.conbuildmat.2023.133766.

[17] C. Cao, W. Xuan and W. Qi. (2023). Zeolites synthesized from industrial and agricultural solid waste and their applications: A review. Journal of Environmental Chemical Engineering. https://doi.org/10.1016/j.jece.2023.110898.

[18] H. Yuan, S. Tang and S. Yin. (2021). Research progress on green synthesis of various high-purity zeolites from natural material-kaolin. Journal of Cleaner Production. https://doi.org/10.1016/j.jclepro.2021.127248.

[19] S.M. Ho and M. Saad. (2023). Review on heavy metal and dye removal via activated carbon adsorption process. Asian Journal of Chemistry. 35: 1-16.

[20] S.M. Ho. (2022). Low-Cost Adsorbents for the Removal of Phenol/Phenolics, Pesticides, and Dyes from Wastewater Systems: A Review. Water. https://doi.org/10.3390/w14203203.

[21] W. Low, W. Lim and H. Lee. (2023). Removal of copper, chromium, and nickel ions from aqueous solution by using different pre-treated orange peel. IOP Conference Series: Earth and Environmental Science. doi:10.1088/1755-1315/1205/1/012013.

[22] S.M. Ho, M. Akram, A. Rashid and U. Laila. (2022). Uses of activated carbon in medicine area: short review. EPRA International Journal of Research and Development. 7: 4-39.

[23] S. Mitali and P. Kumar. (2006). Use of fly ash for the removal of phenol and its analogues from contaminated water. Waste Management. 26, 559-570.

[24] L. Ma, Q. Wang and M. Saiful. (2016). Highly Selective and Efficient Removal of Heavy Metals by Layered Double Hydroxide Intercalated with the MoS_4^{2-} Ion. Journal of the American Chemical Society. 138: 2858-2866.

[25] S. Ahmadi and A. Igwegbe. (2018). Adsorptive removal of phenol and aniline by modified bentonite: adsorption isotherm and kinetics study. Applied Water Science. https://doi.org/10.1007/s13201-018-0826-3.

[26] A. Laura, S. Maria and G. Ana. (2023). Adsorption of Arsenic, Lead, Cadmium, and Chromium Ions from Aqueous Solution Using a Protonated Chabazite: Preparation, Characterization, and Removal Mechanism. Adsorption Science & Technology. https://doi.org/10.1155/2023/2018121.

[27] K. Barbara, S. Nikola and N. Rajic. (2021). Use of Natural Clinoptilolite in the Preparation of an Efficient Adsorbent for Ciprofloxacin Removal from Aqueous Media. Minerals. https://doi.org/10.3390/min11050518.

[28] I. Amir, J. Rahat and Q. Fei. (2022). Application of Attapulgite Clay-Based Fe-Zeolite 5A in UV-Assisted Catalytic Ozonation for the Removal of Ciprofloxacin. Journal of Chemistry. https://doi.org/10.1155/2022/2846453.

[29] S. Rakshit, D. Sarkar and E. Elzinga. (2013). Mechanisms of ciprofloxacin removal by nano-sized magnetite. Journal of Hazardous Materials. 246–247: 221–226.

[30] J. Ma, M. Yang and F. Yu. (2015). Water-enhanced removal of ciprofloxacin from water by porous graphene hydrogel. Scientific Reports. 5: 13578.

[31] E. El-Shafey, H. Al-Lawati and S. Al-Sumari. (2012). Ciprofloxacin adsorption from aqueous solution onto chemically prepared carbon from date palm leaflets. Journal of Environmental Sciences (China). 24: 1579–1586.

[32] R. Cheng, H. Li and Z. Liu. (2018). Halloysite nanotubes as an effective and recyclable adsorbent for removal of low-concentration antibiotics ciprofloxacin. Minerals. 8: 387.

[33] A. Najafpoor, O. Sani and H Alidadi. (2019). Optimization of ciprofloxacin adsorption from synthetic wastewater using γ-Al_2O_3 nanoparticles: An experimental design based on response surface methodology. Colloids and Interface Science Communications, 33: 100212.

[34] H. Fan, Y. Ma and J. Wan. (2020). Adsorption properties and mechanisms of novel biomaterials from banyan aerial roots via simple modification for ciprofloxacin removal. Science of the Total Environmental. 708: 134630.

[35] A. Ashiq, B. Sarkar and N. Adassooriya. (2019). Sorption process of municipal solid waste biochar-montmorillonite composite for ciprofloxacin removal in aqueous media. Chemosphere. 236: 124384.

[36] L. Zhang, G. Qiao and F. Zhao. (2011). Thermodynamic and kinetic parameters of ciprofloxacin adsorption onto modified coal fly ash from aqueous solution. Journal of Molecular Liquids. 163: 53–56.

[37] C. Ngeno, V. Shikuku and F. Orata. (2019). Caffeine and ciprofloxacin adsorption from water onto clinoptilolite: Linear isotherms, kinetics, thermodynamic and mechanistic studies. South African Journal of Chemistry. 72: 139–142.

[38] D. Zide, O. Fatoki and O. Oputu. (2018). Zeolite 'adsorption' capacities in aqueous acidic media; The role of acid choice and quantification method on ciprofloxacin removal. Microporous and Mesoporous Materials. 255: 226–241.

[39] I. Aranaz, B. Elorza and A. Heras. (2021). Chitosan: An Overview of Its Properties and Applications. Polymers. https://doi.org/10.3390/polym13193256.

[40] H. Endar, Y. Seiichiro and M. Yoshiharu. (2022). Methylene Blue Removal by Chitosan Cross-Linked Zeolite from Aqueous Solution and Other Ion Effects: Isotherm, Kinetic, and Desorption Studies. Adsorption Science & Technology. https://doi.org/10.1155/2022/1853758.

[41] S. Radoor, J. Karayil and A. Jayakumar. (2021). Removal of Methylene Blue Dye from Aqueous Solution using PDADMAC Modified ZSM-5 Zeolite as a Novel Adsorbent. Journal of Polymers and the Environment. 29: 3185–3198.

[42] M. Zemedkun, Y. Ayele and T. Dinbore. (2021). Removal of methylene blue from textile waste water using kaolin and zeolite-x synthesized from Ethiopian kaolin. Environmental analysis, Health and Toxicology. doi: 10.5620/eaht.2021007.

[43] M. Tumolo, F. Vito and D. Paola. (2020). Chromium Pollution in European Water, Sources, Health Risk, and Remediation Strategies: An Overview. International Journal of Environmental Research and Public Health. https://doi.org/10.3390/ijerph17155438.

[44] A. Tonni, A. Anouzla and M. Hafiz. (2023). Chromium Removal from Aqueous Solution Using Natural Clinoptilolite. Water. https://doi.org/10.3390/w15091667.

[45] M. Kouli, G. Banis and G. Maria. (2020). A Study on Magnetic Removal of Hexavalent Chromium from Aqueous Solutions Using Magnetite/Zeolite-X Composite Particles as Adsorbing Material. International Journal of Molecular Sciences. https://doi.org/10.3390/ijms21082707.

[46] A. Katsoyiannis, M. Xanthopoulou and A. Zouboulis. (2020). Cr(VI) Femoval from Ground Waters by Ferrous Iron Redox-Assisted Coagulation in a Continuous Treatment Unit Comprising a Plug Flow Pipe Reactor and Downflow Sand Filtration. Applied Sciences, 10: 802.

[47] K. Dermentzis, A. Christophoridis and E. Valsamidou. (2011). Removal of hexavalent chromium from electroplating wastewater by electrocoagulation with iron electrodes. Global NEST Journal. 13: 412–418.

[48] P. Mtimunye, B. Lutsinge and P. Molokwane. (2017). Cr(vi) remediation in groundwater aquifer media using natural organic matter as carbon source. Chemical Engineering Transactions. 61: 1831–1836.

[49] M. Asri, A. Elabed and N. Tirry. (2017). Correlation between cell surface physicochemical properties of bacterial strains and their chromium removal potential. Journal of Adhesion Science and Technology. 31: 2730–2740.

[50] T. Srinath, T. Verma and P. Ramteke. (2002). Chromium (VI) biosorption and bioaccumulation by chromate resistant bacteria. Chemosphere. 48: 427–435.

[51] G. Suresh and B. Babu. (2008). Removal of Cr(VI) from Wastewater using Fly ash as an Adsorbent. Proceedings of International Symposium & 61st Annual Session of IIChE in association with International Partners (CHEMCON-2008), Panjab University, Chandigarh.

[52] C. Yanan, D. An and J. Gao. (2018). Reduction and Removal of Chromium VI in Water by Powdered Activated Carbon. Materials (Basel). doi: 10.3390/ma11020269.

[53] P. Jung, J. Shin and W. Oh. (2022). Removal of Hexavalent Chromium(VI) from Wastewater Using Chitosan-Coated Iron Oxide Nanocomposite Membranes. Toxics. doi: 10.3390/toxics10020098.

[54] P. Panneerselvam, V. Sathya and S. Sivanesan. (2009). Removal of Nickel (II) from Aqueous Solutions by Adsorption with Modified ZSM- 5 Zeolites. E-Journal of Chemistry. 6: 729-736 (2009).

[55] A. Ahmad and E. Ribhi. (1997). Removal of Lead and Nickel Ions Using Zeolite Tuff. Journal of Chemical Technology and Biotechnology. 69: 27-34 (1997).

[56] A. Reyad and E. Aiman. (2012). Removal of cobalt and nickel from wastewater by using Jordan low-cost zeolite and bentonite. Journal of the University of Chemical Technology and Metallurgy. 47: 69-76 (2012).

[57] M. Norfazilah, A. Azian and J. Jaafar. (2018). Removal of nickel from aqueous solution using supported zeolite-Y hollow fiber membranes. Environmental Science and Pollution Research International. 25: 19054-19064.

[58] B. Lidia, F. Małgorzata and M. Jarosław. (2020). Zeolites in Phenol Removal in the Presence of Cu(II) Ions—Comparison of Sorption Properties after Chitosan Modification. Materials. doi:10.3390/ma13030643.

[59] C. Ucan, M. Abatal and A. Miguel. (2019). Removal of an Ethoxylated Alkylphenol by Adsorption on Zeolites and Photocatalysis with TiO_2/Ag. Processes. doi:10.3390/pr7120889.

[60] K. Ayse. (2007). Removal of phenol and 4-chlorophenol by surfactant-modified natural zeolite. Journal of Hazardous Materials. 144: 307-315.

[61] P. Huong, B. Lee and J. Kim. (2016). Improved removal of 2-chlorophenol by a synthesized Cu-nano zeolite. Process safety and Environmental Protection. 100: 272-280.

[62] A. Özgür and C. Ferhan. (2009). Cometabolic bioregeneration of activated carbons loaded with 2-chlorophenol. Bioresource Technology. 100: 4604–4610.

[63] Z. Rawajfih and N. Nsour. (2006). Characteristics of phenol and chlorinated phenols sorption onto surfactant-modified bentonite. Journal of Colloid and Interface Science. 298: 39–49.

[64] K. Rao, S. Singh and R. Singh. (2014). Synthesis and characterization of surface modified graphene–zirconium oxide nanocomposite and its possible use for the removal of chlorophenol from aqueous solution. Journal of Environmental Chemical Engineering. 2: 199–210.

[65] A. Kuleyin. (2007). Removal of phenol and 4-chlorophenol by surfactant modified natural zeolite. Journal of Hazardous Materials. 144: 307–315.

[66] B. Shah, R. Tailor and A. Shah. (2011). Sorptive sequestration of 2-chlorophenol by zeolitic materials derived from bagasse fly ash. Journal of Chemical Technology and Biotechnology. 86: 1265–1275.

[67] A. Imessaoudene, S. Cheikh and J. Bollinger. (2022). Zeolite Waste Characterization and Use as Low-Cost, Ecofriendly, and Sustainable Material for Malachite Green and Methylene Blue Dyes Removal: Box–Behnken Design, Kinetics, and Thermodynamics. Applied Sciences. https://doi.org/10.3390/ app12157587 (2022).

[68] A. Moussa and M. Trari. (2023). Contribution of zeolite to remove malachite green in aqueous solution by adsorption processes: Kinetics, isotherms and thermodynamic studies. Textile Research Journal. https://doi.org/10.1177/00405175231165336.

[69] K. Porkodi and K. Kumar. (2007). Equilibrium, kinetics and mechanism modeling and simulation of basic and acid dyes sorption onto jute fiber carbon: Eosin yellow, malachite green and crystal violet single component systems. Journal of Hazardous Materials. 143: 311-327.

[70] C. Tsai, A. Patel and S. Hsieh. (2022). Engineered mesoporous biochar derived from rice husk for

efficient removal of malachite green from wastewaters. Bioresource Technology. https://doi.org/10.1016/j.biortech.2022.126749.

[71] Y. Mengyuan, C. Ce and L. Dai. (2022). Porous activated carbons derived from bamboo pulp black liquor for effective adsorption removal of tetracycline hydrochloride and malachite green from water. Water Science & Technology. 86: 244–260.

[72] G. Crini, N. Harmel and C. Robert. (2007). Removal of C.I. Basic Green 4 (Malachite Green) from aqueous solutions by adsorption using cyclodextrin-based adsorbent: Kinetic and equilibrium studies. Separation and Purification Technology, 53, 97-110.

[73] S. Ashish, S. Sanjay and V. Vikas. (2017). Removal of malachite green dye from aqueous solution with adsorption technique using Limonia acidissima (wood apple) shell as low cost adsorbent. Arabian Journal of Chemistry. 10: S3229-S3238.

[74] S. Nilay and K. Barun. (2013). Utilization of Sugarcane Baggase, an Agricultural Waste to Remove Malachite Green Dye from Aqueous Solutions. Journal of Materials and Environmental Science. 4: 1052-1065.

[75] A. Baybars. (2016). Isotherm, kinetic, and thermodynamic studies on the adsorption behavior of malachite green dye onto montmorillonite clay. Particulate Science and Technology. 34: 118-126.

[76] M. Baek, D. Kim and O. Se. (2010). Removal of Malachite Green from aqueous solution using degreased coffee bean. Journal of Hazardous Materials. 176: 820-828.

[77] M. Rohani, A. Ali and A. Anis. (2021). Removal of Malachite Green Dye Using Oil Palm Empty Fruit Bunch as a Low-Cost adsorbent. Biointerface Research in Applied Chemistry. 11: 14998-15008.

[78] R. Dibya and M. Hara. (2021). Removal of malachite green dye from aqueous solution using reduced graphene oxide as an adsorbent. Materials Today Proceedings. 47: 1173-1182.

[79] Y. Abate, A. Alene and T. Habte. (2020). Adsorptive removal of malachite green dye from aqueous solution onto activated carbon of Catha edulis stem as a low-cost bio-adsorbent. Environmental Systems Research. https://doi.org/10.1186/s40068-020-00191-4.

[80] M. Abewaa, A. Mengistu and T. Takele. (2023). Adsorptive removal of malachite green dye from aqueous solution using Rumex abyssinicus derived activated carbon. Scientific Reports, https://doi.org/10.1038/s41598-023-41957-x.

[81] E. Oyelude, M. Awudza and K. Twumasi. (2018). Removal of malachite green from aqueous solution using pulverized teak leaf litter: equilibrium, kinetic and thermodynamic studies. Chemistry Central Journal. https://doi.org/10.1186/s13065-018-0448-8.

[82] L. Linh, E. Usama and F. Eiji. (2012). Evaluation of adsorptive removal of Malachite Green from aqueous solutions using Hevea Brasiliensis. International Journal of Biomass & Renewables. 1: 32-38.

[83] Z. Sayed, K. Ali and N. Sayedeh. (2014). Removal of Pb(II) ions and malachite green dye from wastewater by activated carbon produced from lemon peel. Quimica Nova. https://doi.org/10.5935/0100-4042.20140129.

[84] M. Abbas. (2020). Experimental investigation of activated carbon prepared from apricot stones material (ASM) adsorbent for removal of malachite green (MG) from aqueous solution. Adsorption Science & Technology. https://doi.org/10.1177/0263617420904476.